

# Integrating Micro and Nanoscale Materials Processing into the Core ChE Curriculum - Examples in Radiation Heat Transfer

Milo D. Koretsky

Department of Chemical Engineering  
Oregon State University  
Corvallis, OR 97331-2702

## Introduction

The chemical engineering department at Oregon State University (OSU) is committed to developing strength in microelectronics processing within a context of the fundamental skills of the discipline. In this vein, we are integrating examples from this industry into the classroom and the laboratory.<sup>1</sup> These topics are not only useful towards the microelectronics industry but also in the emerging field of nanoscale materials processing. The lab modules, which provide students with hands-on learning as well as more open-ended problem solving experiences, are described elsewhere.<sup>1,2</sup> Another important component to this approach is providing students applications in the context of their core ChE engineering science classes. The classroom examples provide students an integrated experience throughout their undergraduate studies and allow students to synthesize chemical engineering science fundamentals applied toward microelectronics and nanomaterials processes. In this paper, two such examples are presented to illustrate how unit operations from microelectronics processes are integrated into a core engineering science class: (i) substrate heating during sputtering and (ii) estimation of maximum pull rates during Czochralski growth. These examples involve radiation heat transfer and can be applied to a transport phenomena (heat transfer) class. Similar examples are being introduced in material and energy balances, fluids, mass transfer, thermodynamics and chemical reaction engineering. The objective of this paper is to demonstrate how these “non traditional” examples have been incorporated as core ChE engineering science topics at OSU, and provide two examples which can be used in a transport phenomena / heat transfer class.

Hundreds of individual process steps are used in the manufacture of even simple microelectronics devices. However, the fabrication sequence uses many of the same *unit operations* numerous times. These unit operations rely on core chemical engineering science. Modules of many unit operations have been developed for integration into the chemical engineering curriculum and unit operations laboratory at OSU. In addition to the processes discussed in this paper, these modules include: plasma etching, chemical vapor deposition, spin coating, electrochemical deposition, silicon oxidation, and chemical mechanical planarization.<sup>1</sup> Such unit operations contain complex systems that involve the interaction of many physical and chemical processes. However, when these unit operations are covered at the university, they are often taught in survey courses and approached descriptively and phenomenologically. An

alternative approach is to understand these processes in terms of fundamental principles covered in the chemical engineering curriculum. A correlation of specific unit operations to chemical engineering fundamentals is depicted in Table 1. By developing classroom examples in this manner, these unit operations, are rendered more accessible, including those providing hands-on learning in the lab. At the same time, a greater depth is provided to undergraduate chemical engineers by reinforcing the fundamental engineering science taught in the curriculum.

**Table 1.** Unit Operations in Microelectronic Device Fabrication

Unit Operations	Chemical Engineering Core Courses	Unit Operations	Chemical Engineering Core Courses
Bulk Crystal Growth from Melt	Fluid Dynamics Heat Transfer Mass Transfer Thermodynamics Process Control	Lithography Photoresist spin coating Photoresist baking Photoresist exposure and development	Fluid Dynamics Mass Transfer Polymer Rheology Kinetics Process Control
Surface Reactions Cleaning Oxidation	Kinetics Fluid Dynamics Mass Transfer	Doping and Dopant Redistribution Ion implantation Thermal diffusion	Mass Transfer Heat Transfer Process Control
Etching Plasma Etching Wet Etching	Fluid Dynamics Mass Transfer Kinetics Reaction Engineering Process Control		
Thin Film Deposition Sputtering Physical Vapor Deposition Chemical Vapor Deposition Electrochemical Deposition	Kinetics Fluid Dynamics Mass Transfer Heat Transfer Thermodynamics Electrochemical Engineering Reaction Engineering Process Control	Planarization Chemical Mechanical Planarization	Fluid Dynamics Mass Transfer Electrochemical Engineering Process Control

Drawing on ideas from John Dewey, Kurt Lewin and Jean Piaget, David Kolb models the learning process in terms of an experiential learning cycle.<sup>3</sup> As schematically shown in Figure 1, there are four stages of learning that follow one another: concrete experience, reflective observation, abstract conceptualization, and active experimentation. Two of these stages, concrete experience and abstract conceptualization, operate in the realm of knowing (how we perceive) while the other two, reflective observation and active experimentation, involve transformation of knowledge. It is by perceiving and then transforming knowledge that we learn. The most effective instruction ensures that learning activities give full attention, in order, to each quadrant of this cycle. While it can be argued this model is a simplification of the complex learning process, it forms a useful basis from which to construct learning materials. Curricular materials can be made more effective by leading the student through successive stages of the cycle. In fact, the Department of Chemical Engineering's ABET assessment process at OSU has been developed around Kolb's learning cycle. The radiation heat transfer examples are presented in the context of Kolb's learning cycle: (i) the physical process is described and application in

industry briefly illustrated (concrete experience); (ii) the qualitative behavior of the system is discussed/predicted (reflective observation); (iii) asymptotic and/or analytical solutions are developed (abstract conceptualization); and (iv) discussion of solutions obtained and their implication and extrapolation to industrial process engineering (active experimentation). Several of the activities described below will be specifically connected to Kolb's cycle.

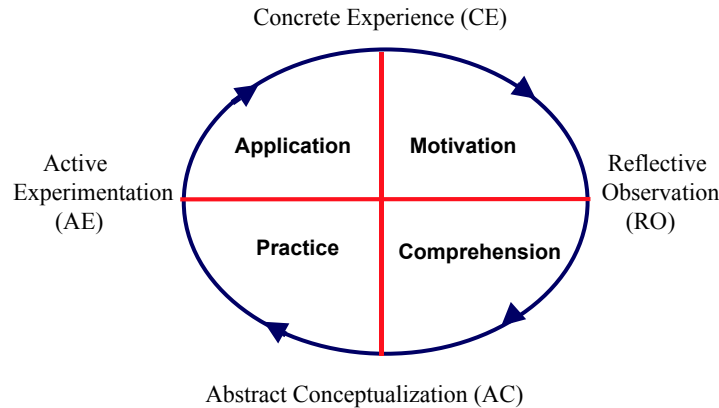


**Figure 1.** The Kolb cycle of experiential learning

### Energy Balance with Radiation:

In classic transport phenomena courses, conductive and convective heat transfer are usually emphasized over radiation. In fact, while radiation is presented as one of the three modes of heat transfer (along with convection or conduction); it is often either not illustrated by example or only included in a “stand alone” chapter and not integrated into the other course materials.<sup>4,5</sup> However, radiation can be an important heat transfer mechanism not only for processes which occur at high temperature but also in vacuum systems where the effect of convection and conduction are diminished. Both these cases are encountered in the Microelectronics Unit Operations described in Table 1. Thus, there is a good opportunity to illustrate applications where it is appropriate to include the radiation term in the energy balance.

Accounting for convection with a heat transfer coefficient,  $h$ , and generation with the term  $\dot{G}$ , the unsteady energy balance in one ( $z$ ) dimension, including radiation, can be written:

$$\rho c_v V \frac{\partial T}{\partial t} = V \frac{\partial}{\partial z} \left[ k \frac{\partial T}{\partial z} \right] - hA(T - T_w) - \sigma \varepsilon A (T^4 - T_w^4) + \dot{G} \quad (1)$$

Equation (1) allows the calculation of temperature,  $T$ , with time,  $t$ , and position,  $z$ . Other symbols are defined in Table 2. In the examples that follow, no attempt is made to account for radiation view-factors for which detailed geometry is needed.

**Table 2.** Explanation of nomenclature and typical values for heat transfer analysis.

Symbol	Description	Units	Value
$A$	Area across which heat transfer process occurs	$m^2$	
$c_v$	Heat capacity at constant volume	J / (g K)	0.7 for Si
$d$	Substrate thickness	cm	0.076
$\dot{G}' = \frac{\dot{G}}{A}$	Energy generation flux to the substrate	J / (cm <sup>2</sup> s)	Calculated
$g_1$	Enthalpy of sublimation	eV / atom	3.4 for Al
$g_2$	Kinetic energy of sputtered atoms	eV / atom	6 for Al
$g_3$	Radiation emitted by the plasma	eV / atom	4 for Al
GR	Growth rate	$\mu m / min$	1.0
$k$	Thermal conductivity	J / (cm s K)	0.22 for Si at $T_m$
$T_0$	Initial substrate temperature	K	298
$T_m$	Melting temperature	K	1687 for Si
$T_w$	Wall temperature	K	298
$T_\infty$	Temperature after a long time	K	Calculated
$V$	Volume of control element	$m^3$	
$\Delta h_{fus}$	Enthalpy of fusion	KJ/mol	-50.2 for Si
$\varepsilon$	Emissivity	unitless	0.09 for Al 0.46 for Si 0.93 for SiO <sub>2</sub>
$\rho$	Density	$g / cm^3$	2.7 for Al 2.33 for Si 2.2 for SiO <sub>2</sub>
$\sigma$	Stefan-Boltzmann constant	J / (cm <sup>2</sup> s K <sup>4</sup> )	$5.68 \times 10^{-12}$

**Example 1: Substrate Heating during Sputtering**

Sputtering is a plasma-based process used to deposit thin films.<sup>6,7</sup> A sputtering plasma is a weakly ionized gas, containing a small amount of electrons and ions (1-100 ppm) in addition to neutrals.<sup>8</sup> Typically, argon is used as the sputtering gas. The gas phase species include neutral argon in the ground state (Ar) and excited electronic states (Ar<sup>\*</sup>), argon ions (Ar<sup>+</sup>), and free electrons (e<sup>-</sup>). The excited-state argon can radiatively decay emitting the light which gives the

plasma its characteristic *glow*. A schematic of a sputtering process is shown in Figure 2. The process occurs under vacuum, typically around 10 mtorr. A solid material of the same composition of the film that is to be deposited, the *target*, is placed on one electrode in the plasma while the substrate is placed on the other electrode. Energetic ions bombard the *target* displacing, or sputtering, atoms from the solid. The sputtered atoms leave the target with significant kinetic energies, from around 1-30 eV and transport across the plasma where they impinge on a substrate and can be incorporated into the growing film. In this process, the precursors to film growth are generated from the solid target, in contrast to plasma enhanced chemical vapor deposition where dissociated gas phase species lead to film growth. More details on the sputtering process can be found in refs 6-8.

The temperature at the substrate affects the structure and properties of the deposited film since various elementary processes such as adsorption, desorption, surface diffusion and chemical reaction depend critically on temperature. The resultant film structures can range from columnar to equiaxed to amorphous. An energy balance on the substrate can be used to estimate its temperature and is an illustrative example of how a time dependent heat transfer calculation can be used to evaluate an important reactor parameter.

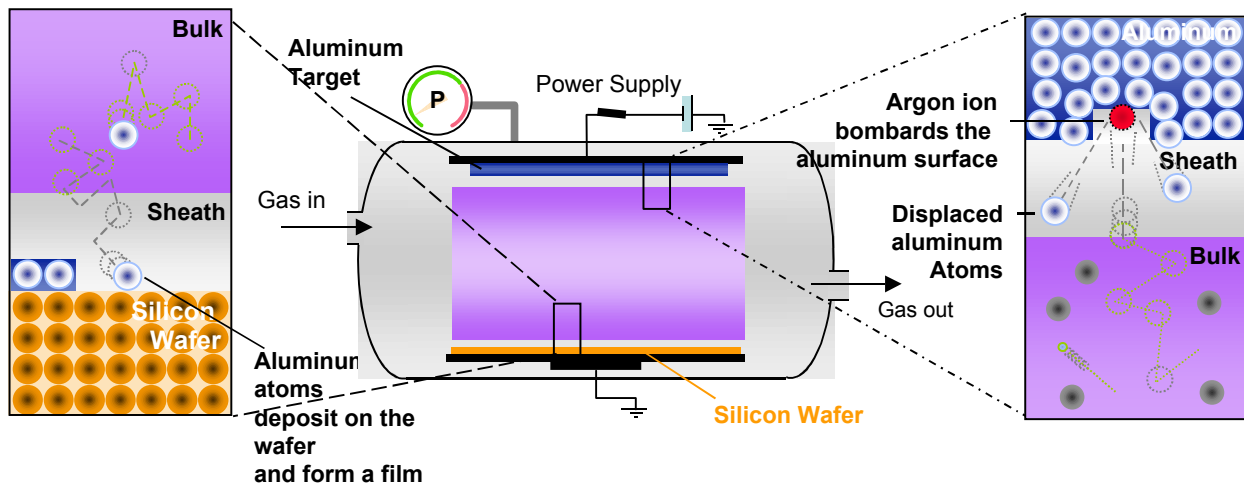


**Figure 2.** Schematic of a sputtering plasma. The inset on the left illustrates the growth process on the plasma surface; the inset on the right illustrates the “sputtering” of the Al target.

Three components are considered for the generation of heat at the wafer surface: the latent heat of condensation, the kinetic energy on the incoming sputtered atoms, and the radiation from the *glow* of the plasma. These terms are labeled  $g_i$ , in units of [eV/atom]. They are quantified as follows:

1. The enthalpy of sublimation,  $\Delta h_{sub}$  can be obtained from thermodynamic data; for example, using the enthalpy of formation for aluminum gas at 298 K of 329.7 kJ/mol<sup>9</sup>, a value for  $g_1$  can be obtained:  $g_1 = \Delta h_{sub} = 3.4 \left[ \frac{\text{eV}}{\text{atom}} \right]$ .

2. The kinetic energy of sputtered atoms. While theory predicts the average kinetic energy of the incoming particles is  $(\Delta h_{sub}/2)$ ,<sup>10</sup> measured values are considerably higher.<sup>11</sup> A value  $g_2 = \Delta ke = 6 \left[ \frac{\text{eV}}{\text{atom}} \right]$  is used for Al.<sup>11</sup>
3. Plasma radiation itself (as apposed to thermal radiation from a hot surface). This contribution comes from relaxation of exciting species that give the plasma its *glow*. This component is system dependent, depends on the plasma physics and is complicated to characterize. We use the reported value of
 
$$g_3 = h\nu_{plasma} = 4 \left[ \frac{\text{eV}}{\text{atom}} \right]_{10}$$

We next consider processes by which the substrate can lose energy. We assume there is no wafer cooling. We also assume the substrate is thermally isolated from the substrate holder, so that all heat transfer processes occur within the vacuum system. These conditions represent the limiting case where the increase in temperature is the greatest; in fact, if the temperature change so calculated is too large, a substrate cooling system can be designed into the sputtering system. Since the process occurs at such low pressure, e.g., 10 mtorr, conduction and convection can be neglected; therefore, the primary heat transfer mechanism is radiation. No attempt is made to account for view-factors which depend on the specific geometry of the sputtering system. Since the volume of the wafer is  $\pi R^2 d$  and the heat transfer occurs across the area  $\pi R^2$ , Equation (1) is reduced to:

$$\rho c_v d \frac{dT}{dt} = \dot{G}' - \sigma \varepsilon (T^4 - T_w^4) \quad (2)$$

where  $d$  is the thickness of the silicon wafer and  $\dot{G}' = \frac{\dot{G}}{A}$  is the energy flux of generation. Except for the small film deposited on the top, the substrate material is silicon; therefore, the properties of silicon are used. Since the thermal conductivity of silicon is large, the wafer itself can be treated by “lumped-parameter” analysis and assigned a uniform temperature,  $T$ .

First, two asymptotes of the solution are considered, short time vs. long time. In the asymptotic limit of short time, dissipation by radiation is negligible and the energy balance reduces to:

$$\rho c_v d \frac{dT}{dt} = \dot{G}' \quad (3)$$

Applying the initial condition, at  $t = 0$ ,  $T = T_0$ , integration of Equation (3) gives:

$$T = T_0 + \frac{\dot{G}'}{d\rho c_v} t \quad (4)$$

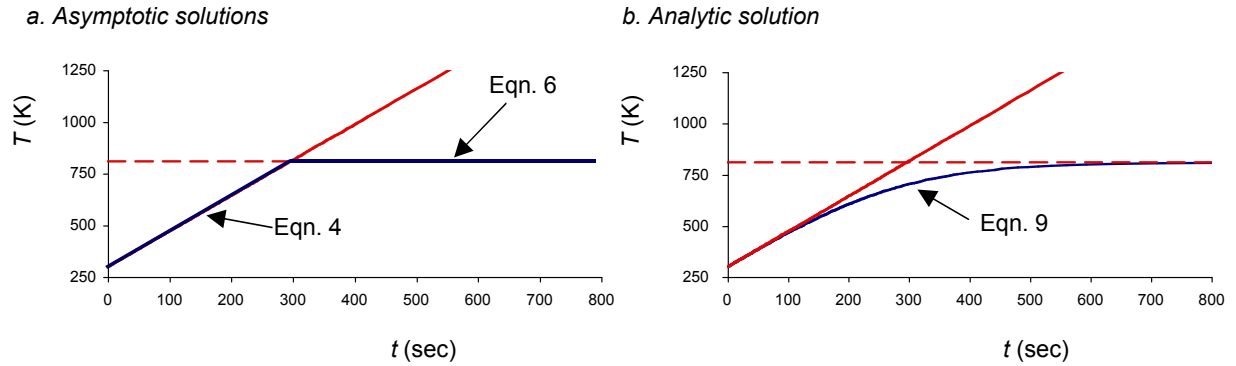


**Figure 3** **a.** Asymptotic solutions of the substrate temperature at short [Equation (4)] and long [Equation (6)] times. **b.** Analytic solution of given by Equation (9).

Inspection of Equation (4) shows that the temperature increases monotonically with time and is unbounded. This problem is solved quantitatively for Al using the estimate for  $\dot{G}'$  given above. Most of the uncertainty of this analysis lies in this estimate. This asymptotic case is shown in Figure 3a, labeled “Eqn. 4”.

The other asymptotic limit occurs at steady state, where  $\frac{dT}{dt} = 0$  and  $T = T_\infty$ :

$$0 = \dot{G}' - \sigma\varepsilon(T_\infty^4 - T_w^4) = \left(\dot{G}' + \sigma\varepsilon T_w^4\right) - \sigma\varepsilon T_\infty^4 \quad (5)$$

Solving Equation (5) for  $T_\infty$  gives

$$T_\infty = \left(\frac{\dot{G}' + \sigma\varepsilon T_w^4}{\sigma\varepsilon}\right)^{1/4} \quad (6)$$

The solution to the steady-state asymptotic limit is shown in Figure 3a, labeled “Eqn. 6”. These two cases bound the limits for the substrate temperature as shown by the blue curve in Figure 3a.

Once the limiting cases have been shown, the complete analytical solution is presented. We can rewrite Equation (2):

$$\frac{dT}{dt} = a^2 - b^2 T^4 \quad (7)$$

where

$$a^2 = \frac{\dot{G}' + \sigma\varepsilon T_w^4}{d\rho_{Si}c_{v,Si}} \quad \text{and} \quad b^2 = \frac{\sigma\varepsilon}{d\rho_{Si}c_{v,Si}} \quad (8)$$

Integrating Equation (7) with the initial condition, at  $t = 0$ ,  $T = T_0$ , gives an implicit relation for temperature. Appendix A provides details of the integration.

$$t = \frac{1}{4a^{3/2}b^{1/2}} \left\{ \ln \left( \frac{(\sqrt{a} - \sqrt{b}T_0)(\sqrt{a} + \sqrt{b}T)}{(\sqrt{a} - \sqrt{b}T)(\sqrt{a} + \sqrt{b}T_0)} \right) + 2 \left[ \tan^{-1} \left( \sqrt{\frac{b}{a}} T \right) - \tan^{-1} \left( \sqrt{\frac{b}{a}} T_0 \right) \right] \right\} \quad (9)$$

The analytical solution is shown in Figure 3b, and can be seen to fit in nicely to the asymptotic solutions in Figure 3a. The use of limiting solutions is illustrated by solving for substrate temperature in this manner. Indeed the behavior of systems for which an analytical solution is not tractable can be approximated in this way.

Once the substrate temperature for Al has been shown, students are asked a qualitative “process engineering” question, in which they are required to synthesize this information. This exercise allows them to tie back to the application quadrant of the Kolb learning cycle. “If your manager wanted you to change the deposited film from Al to SiO<sub>2</sub>, would you need to worry about designing a heater for your substrate?” Table 1 shows some parameters for SiO<sub>2</sub>. While the generation terms will be of similar magnitude, the emissivity of the oxide is an order of magnitude greater than the Al metal. This leads to more effective cooling by radiation so the temperature does not rise as quickly. Indeed solution shows the maximum temperature to be only 388 K.

### Example 2: Maximum Pull Rate during Single Crystal Growth

Solid state devices have become ubiquitous in everyday life. Single crystal silicon is used as the substrate material in all but a few niche applications. Industrially, these single crystals are almost exclusively grown by the Czochralski (CZ) method. Silicon and other semiconductors that are used as substrates for electronic materials processing have stringent materials requirements in terms of both chemical purity and crystal structure. For example silicon must be an extremely pure (10 ppm impurity), dislocation-free single crystal. There are three major steps in the manufacture of silicon wafers for integrated circuit processing: (i) production of 99.999999999% pure Si (EGS); (ii) growth of a single crystal cylindrical silicon boule from the melt; and (iii) slicing and polishing the boule into wafers. Presently, silicon wafers typically have 200 or 300 mm diameters. The example presented here illustrates an engineering science example from step (ii) above.

A schematic of the Czochralski growth method is shown in Figure 4a. In the growth process, a suitable oriented seed crystal is placed atop a crucible of molten electronic grade silicon and then slowly pulled, resulting in a cylindrical single crystal Si solid. A small amount of a second species (e.g., B, P, As, In) can be added to the melt as a *dopant* to provide desirable electrical properties. The crucible rotates in one direction, while the Si boule rotates in the other. The solid-liquid interface must be maintained very close to the melting point for single crystal growth to be achieved. For silicon, the interface is maintained at 1687 K. For more details of the growth process, see refs 12-14. The CZ growth process is rich with application of chemical engineering science<sup>15</sup> including thermodynamics (liquid-solid phase equilibria, distribution of dopant and

impurity at interface), mass transfer (dopant concentration distribution in the boule)<sup>16</sup> and the radiation heat transfer example discussed below.

The production rate of silicon by the CZ method is limited by the velocity that the crystal can be pulled from the melt. Industrial growth rates take up to 2 days. The interface temperature must remain constant to achieve single crystal growth; therefore, the latent enthalpy of fusion associated with the solidification of silicon must be dissipated via heat transfer. If the boule is pulled too fast, the energy released upon crystallization will accumulate at the interface, leading to an increase in temperature and an undesirable polycrystalline solid.

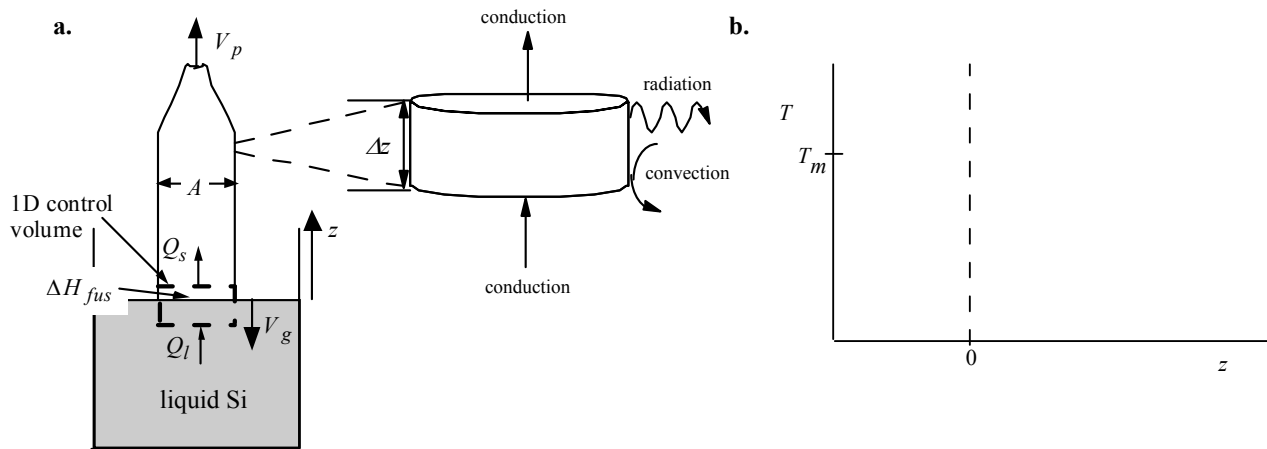


**Figure 4.** a. Schematic of CZ crystal growth from the melt. Control elements depicting the energy transfer processes at the liquid-solid interface and up the solid boule are shown. b. Students are asked to predict the temperature profile before solving the problem.

To get students thinking about the energy balance they are asked to predict the one dimensional temperature profile they expect as shown in Figure 4b. This learning activity corresponds to the Abstract Conceptualization step in the Kolb cycle.

An energy balance can be applied to the liquid-solid interface, to quantify the energy transfer processes and determine the conditions that limit growth velocity. The important terms to consider are illustrated in the 1D control volume at the melt-solid interface in Figure 4a. At steady-state, the enthalpy of fusion  $\Delta h_{fus}$ , must be balanced by the energy transferred into the control volume by heat from the melt,  $\dot{Q}_l$ , and the energy leaving the interface through the solid,  $\dot{Q}_s$ .

$$\dot{n}\Delta h_{fus} = \dot{Q}_l - \dot{Q}_s \quad (10)$$

where  $\dot{n}$  is the solidification rate in mol/s. The solidification rate can be related to the growth rate,  $V_g$ , since the density and molecular weight,  $MW$ , of silicon are known.

$$\dot{n} = \frac{\rho A V_g}{MW} \quad (11)$$

The heat transfer from the melt depends on both conduction and convection, and is an interesting, but non-trivial problem in fluid mechanics.<sup>13,15</sup> However, we can get maximum pull rate if we approximate  $\dot{Q}_l = 0$ . Energy transfers away from the interface and up the solid boule by conduction and can be written as

$$\dot{Q}_s = -kA \left. \frac{dT}{dz} \right|_{z=0} \quad (12)$$

Combining Equations (10), (11) and (12) gives:

$$(V_g)_{\max} = \frac{kMW}{\Delta h_{fus} \rho} \left. \frac{dT}{dz} \right|_{z=0} \quad (13)$$

If we pull the Si faster than  $V_{g, \max}$ , the interface temperature drops and polycrystalline growth is realized.

How do we get  $\left. \frac{dT}{dz} \right|_{z=0}$  in Equation (13)? The growth velocity,  $V_g = \frac{dz}{dt}$ , transforms this

moving boundary problem from a partial differential equation to an ordinary differential equation. Rewriting Equation (1), we get

$$\rho c_P V_g \frac{dT}{dz} = \frac{d}{dz} \left[ k \frac{dT}{dz} \right] - \frac{2\sigma\varepsilon}{R} (T^4 - T_w^4) - \frac{2h}{R} (T - T_w) \quad (14)$$

where the heat transfer processes quantified on the right hand side of Equation (14) are shown in Figure 4a. This equation can be solved numerically.<sup>17</sup> To get an analytical solution, we must make some approximations.

1. We can neglect the accumulation term by realizing that pull rates, i.e.,  $V_p$ , are small and will be negligible compared to axial conduction.
2. The surrounding temperature,  $T_w$ , will be small compared to the boule temperature (at least close to the melt), so we can neglect  $T_w$ .

Typically a third approximation is made; the thermal conductivity is not a function of temperature.<sup>12,18</sup> With these approximations, Equation (14) becomes:

$$0 = k \frac{d^2 T}{dz^2} - \frac{2\sigma\varepsilon}{R} T^4 \quad (15)$$

The temperature at the interface is equal to the melting temperature of silicon. Using this boundary condition at the interface, i.e.,  $z = 0$ ,  $T = T_m$ , the solution to Equation (15) is given by

$$T = \left[ \left( \sqrt{\frac{9\sigma\varepsilon}{5kR}} \right) z + T_m^{-3/2} \right]^{-2/3} \quad (16)$$

and the growth velocity is given by Equation (13)

$$(V_g)_{\max} = -\frac{MW}{\Delta h_{fus}\rho} \sqrt{\frac{4\sigma\varepsilon k}{5R}} T_m^{5/2} \quad (17)$$

A more accurate solution is obtained if we account for the temperature dependence of the thermal conductivity of silicon. In this case, Equation (14) becomes:

$$0 = k(T) \frac{d^2 T}{dz^2} + \frac{dk(T)}{dz} \frac{dT}{dz} - \frac{2\sigma\varepsilon}{R} T^4 \quad (18)$$

Data for the thermal conductivity are shown in Figure 5.<sup>19</sup> A reasonable fit of these data for the temperature dependant thermal conductivity of silicon,  $k(T)$ , is given by:

$$k(T) = \frac{const.}{T} = \frac{k_m T_m}{T} \quad (19)$$

where  $k_m$  is the thermal conductivity at the melting temperature.

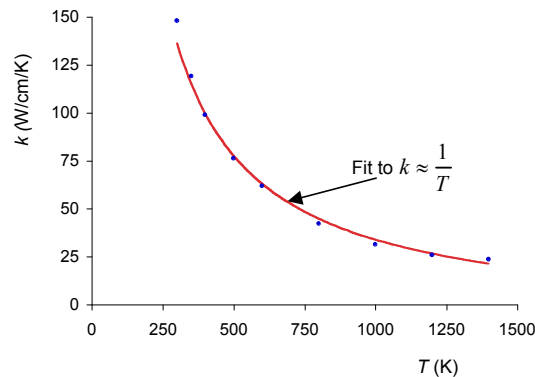


**Figure 5.** Data from ref. 19 for the thermal conductivity of silicon (blue dots) and the fit to  $1/T$  (red curve).

Using the fit given by Equation (19), Equation (18) becomes

$$0 = \frac{k_m T_m}{T} \frac{d^2 T}{dz^2} - \frac{k_m T_m}{T^2} \left( \frac{dT}{dz} \right)^2 - \frac{2\sigma\varepsilon}{R} T^4 \quad (20)$$

The solution to Equation (20) with the boundary condition at  $z = 0$ ,  $T = T_m$ , gives

$$T = \left[ \left( \sqrt{\frac{2\sigma\varepsilon}{k_m T_m R}} \right) z + T_m^{-2} \right]^{-1/2} \quad (21)$$

and

$$(V_g)_{\max} = -\frac{MW}{\Delta h_{fus} \rho_s} \sqrt{\frac{\sigma\varepsilon k_m}{2R}} T_m^{5/2} \quad (22)$$

Comparing the results given by Equations (22) and (17) gives

$$\frac{(V_g)_{\max, k(T)}}{(V_g)_{\max, k=const}} = \sqrt{\frac{5}{8}} = 0.79 \quad (23)$$

These results are compared to experimental data in Figure 6.

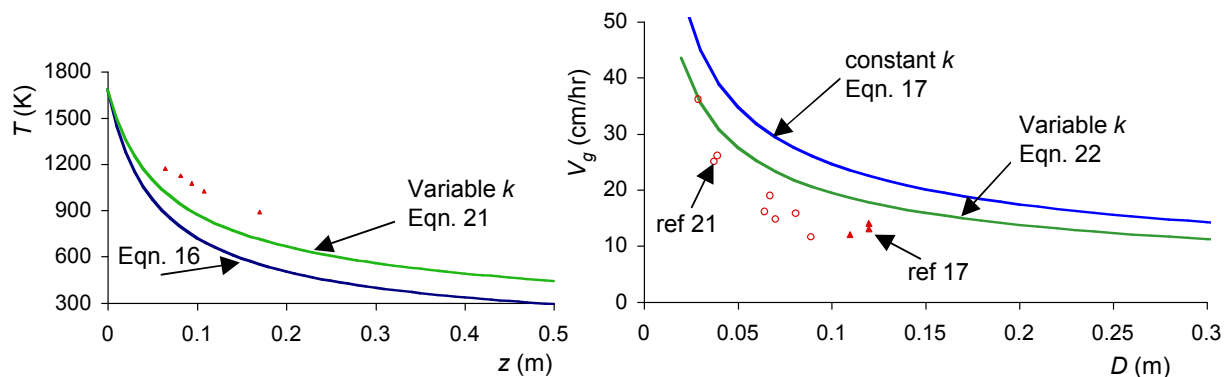


**Figure 6.** **a.** Temperature profile along the Si boule for constant conductivity [Equation (16)] and variable conductivity [Equation (20)]. Experimental data from ref 20 are also shown. **b.** Maximum pull velocity vs. boule diameter. Experimental data from refs 17 and 21 are also shown.

### Assessment

An assessment survey was conducted to seniors graduating in June 2004. Possible scores ranged from a low of 1 (strongly disagree) to a high of 5 (strongly agree). A total of 28 students returned the survey. The results are summarized in Table 3. The overall response is encouraging. In general, students feel that the program in Microelectronics Processing Unit Operations enhances their overall learning (4.42/5.00). They also feel this program better prepares them for industrial practice (4.58/5.00), coinciding with OSU's College of Engineering's mission to make students "work ready". Additionally students feel they are able to adequately apply engineering science to the microelectronics Unit Operations (4.19/5.00). On the other hand, the lowest score received was for the success of integrating these core Unit Operations into the chemical engineering core (3.81/5.00). Contributing factors include: (i) the high cognitive demand on students for this type of curricular integration; (ii) the large "time constant" between implementing the in class changes and having them effectively presented to a graduating senior throughout their entire curriculum; and (iii) the challenge of getting this material into classes taught by faculty with no direct attachment to this initiative. It is hoped that by developing material that is more class-ready, as the examples in this paper, the third factor can be mitigated.

**Table 3.** Assessment of graduating seniors

Question	Score
1. Microelectronics Processing Unit Operations are integrated into OSU's core chemical engineering's curriculum.	3.81
2. I am able to apply fundamental engineering science to Microelectronics Processing Unit Operations.	4.19
3. I believe that the integration of Microelectronics Processing Unit Operations will better prepare me for industrial practice.	4.58
4. I have learned new engineering science from the newly developed Unit Operations Labs in Microelectronics Processing.	4.27
5. Professional practices are effectively incorporated into these Unit Operations Labs in Microelectronics Processing.	4.04
6. Overall, these newly developed Microelectronics Processing Unit Operations Labs enhance my learning at OSU.	4.42

### Acknowledgements

The author is grateful for support provided by the Intel Faculty Fellowship Program and the National Science Foundation's Course, Curriculum and Laboratory Improvement Program under grant DUE-0127175.

## References

1. Milo D. Koretsky, Chih-hung (Alex) Chang, Sho Kimura, Skip Rochefort, and Cyndie Shaner, "Integration of Microelectronics-Based Unit Operations into the ChE Curriculum," Proc. ASEE, Session 1313 (2003).
2. Chih-hung (Alex) Chang, Milo D. Koretsky, Sho Kimura, Skip Rochefort, and Cyndie Shaner, "Lab-Based Unit Operations in Microelectronics Processing," *Chemical Engineering Education*, **37** 188 (2003).
3. Kolb, D.A., *Experiential Learning*, Prentice Hall, New Jersey: 1984.
4. Welty, J.R. C.E. Wicks and R.E. Wilson, *Fundamentals of Momentum, Heat, and Mass Transfer*, 4<sup>th</sup> Ed., Wiley, New York: 2001.
5. Bird, R.B., W.E. Stewart, and E.N. Lightfoot, *Transport Phenomena*, 2<sup>nd</sup> Ed., Wiley, New York: 2002.
6. Chapman, Brian N., *Glow discharge processes: sputtering and plasma etching*, Wiley, New York: 1980.
7. Vossen J.L and J.J. Cuomo, Chapter II-1 in *Thin Film Processes*, J.L Vossen and W Kern, Eds, Academic Press, New York: 1978.
8. For more background material on plasma processes see <http://classes.engr.oregonstate.edu/che/fall2003/che571/Topic5.pdf>
9. Barin, I., *Thermochemical Data of Pure Substances*, Vol. I and II, 3<sup>rd</sup> Ed. VCH, New York: 1995.
10. Kersten, H., H. Deutsch, H. Steffen, G.M.W. Kroesen, and R. Hippler, *Vacuum*, **63** 385 (2001).
11. Thornton, J.A., *Thin Solid Films*, **54** 23 (1978).
12. Liaw, H.M. Chapter 3 in *Handbook of Semiconductor Silicon Technology*, W.C. o'Mara, R.B. Herring and L.P. Hunt, Eds, Noyes Publications, Park Ridge, NJ: 1990.
13. Zulehner, W. and D. Huber, Pages 1-143 in *Silicon, Chemical Etching (Crystals 8 – Growth, Properties, and Applications)*, J. Grabmaier, Ed, Springer-Verlag, Berlin: 1982.
14. For more background material on silicon crystalgrowth see <http://classes.engr.oregonstate.edu/che/fall2003/che571/Topic2.pdf>
15. Brown, R.A., Chapter 2 in *Microelectronics Processing: Chemical Engineering Aspects*, D.W. Hess and K.F. Jensen Eds., American Chemical Society, Washington DC: 1989.
16. Anderson, T.J., Pages 311-333 in *Chemical Engineering Education in a Changing Environment*, S.L. Sandler and B.A. Finlayson, Eds., AIChE Publications, New York: 1988.
17. Rae, S. N. *J. Crystal Growth* **54**, 261 (1981).
18. S. Middleman and A. Hochberg, *Process Engineering Analysis in Semiconductor Device Fabrication*, McGraw-Hill, New York: 1993.
19. Glassbrenner, C. J. and G. A. Slack, *Phys. Rev.* **134**, 4A A1058 (1964).
20. Williams, G. and R.E. Reusser, *J. Crystal Growth* **64**, 448 (1983).
21. Digges, T.G. and R. Shima, *J. Crystal Growth* **50**, 865 (1980).

**Milo D. Koretsky** is an Associate Professor of Chemical Engineering at OSU. He received his BS and MS degrees from UCSD and Ph D from UC Berkeley, all in chemical engineering. Professor Koretsky's research interests are in thin film materials processing including: plasma etching, chemical vapor deposition, electrochemical processes and chemical process statistics. He is author of the book, *Engineering and Chemical Thermodynamics*.

## Appendix A. Integration of Equation (7)

Integrating Equation (7) gives:

$$\int_0^t dt = \int_{T_0}^T \frac{dT}{a^2 - b^2 T^4} = \frac{1}{2a} \int_{T_0}^T \left[ \frac{1}{a - bT^2} + \frac{1}{a + bT^2} \right] dT \quad (\text{A1})$$

To integrate the first term on the right hand side in Equation (A1), we use integration by partial fractions:

$$\begin{aligned} \frac{1}{2a} \int_{T_0}^T \left[ \frac{1}{a - bT^2} \right] dT &= \frac{1}{4a^{3/2}} \int_{T_0}^T \left[ \frac{1}{\sqrt{a} - \sqrt{b}T} + \frac{1}{\sqrt{a} + \sqrt{b}T} \right] dT \\ &= \frac{1}{4a^{3/2}b^{1/2}} \left[ -\ln \left( \frac{\sqrt{a} - \sqrt{b}T}{\sqrt{a} - \sqrt{b}T_0} \right) + \ln \left( \frac{\sqrt{a} + \sqrt{b}T}{\sqrt{a} + \sqrt{b}T_0} \right) \right] \quad (\text{A2}) \\ &= \frac{1}{4a^{3/2}b^{1/2}} \ln \left( \frac{(\sqrt{a} - \sqrt{b}T_0)(\sqrt{a} + \sqrt{b}T)}{(\sqrt{a} - \sqrt{b}T)(\sqrt{a} + \sqrt{b}T_0)} \right) \end{aligned}$$

For the second term, we must use some trigonometry. Since,  $\tan(\tan^{-1} x) = x$  then differentiating with respect to  $x$  gives

$$\sec^2(\tan^{-1} x) \frac{d}{dx}(\tan^{-1} x) = 1 \quad (\text{A3})$$

By the Pythagorean identity

$$\sec^2(\tan^{-1} x) = 1 + \tan^2(\tan^{-1} x) = 1 + x^2 \quad (\text{A4})$$

Substituting Equation (A4) into Equation (A3) and rearranging,

$$\frac{d}{dx}(\tan^{-1} x) = \frac{1}{1 + x^2} \quad (\text{A5})$$

Integrating Equation (A5) gives

$$\int \frac{1}{1 + x^2} dx = \tan^{-1} x \quad (\text{A6})$$

The second term on the right hand side in Equation (A1) can be written

$$\frac{1}{2a} \int_{T_0}^T \left[ \frac{1}{a + bT^2} \right] dT = \frac{1}{2a^{3/2}b^{1/2}} \int_{x_0}^x \left[ \frac{1}{1 + x^2} \right] dx \quad (\text{A7})$$

where

$$x^2 = \frac{b}{a} T^2 \quad (\text{A9})$$

Substituting Equations (A6) and (A8) in Equation (A7) gives

$$\frac{1}{2a} \int_{T_0}^T \left[ \frac{1}{a + bT^2} \right] dT = \frac{1}{2a^{3/2}b^{1/2}} \left[ \tan^{-1} \left( \sqrt{\frac{b}{a}} T \right) - \tan^{-1} \left( \sqrt{\frac{b}{a}} T_0 \right) \right] \quad (\text{A10})$$

Substitution of Equations (A2) and (A10) in (A1) gives Equation (9).